Springer

KSME

Journal of Mechanical Science and Technology 24 (2010) 407~414
www.springerlink.com/content/1738-494x
DOI 10.1007/s12206-009-1113-x

The optimum solidification and crucible rotation in silicon czochralski crystal growth †

Hyomin Jeong[1], Yonghun Lee[2], Myoungkuk Ji[2], Gyeonghwan Lee[3] and Hanshik Chung[1,*]

[1]*Dept. of Mechanical and Precision Engineering The Institute of Marine Industry, Gyeongsang National University, 445 Inpyeong-Dong, Tongyeong, Gyeongsangnamdo,650-160, South Korea*
[2]*Dept. of Mechanical and Precision Engineering, Gyeongsang National University*
[3]*Graduate school, Dept. of Mechanical and Precision Engineering, Gyeongsang National University*

(Manuscript Received January 15, 2009; Revised July 31, 2009; Accepted September 28, 2009)

Abstract

Silicon crystallization is very important in many industrial processes, and it is desirable that maker should have a low cost manufacturing and high efficiency for producing semiconductors. One semiconductor process is the Czochralski (CZ) silicon melt flow and this CZ process has an excellent manufacturing feature and is utilized for silicon solidification. But CZ silicon melt flow is very complicated and this defect can be erased by the numerical analysis of the melt flow. In this paper, the optimum solidification conditions were shown for crucible rotation. This is because the solidification conditions depend on crucible rotation under the cooling process and the solidification conditions were investigated on heat generation rate on crucible wall and rotation by using numerical analysis. For the numerical validations, we verified with experimental data and showed good agreement with current numerical results. The solidification regions are classified with crystal rotation and crucible rotation. For the heat generation rate, qw, the optimum heat generation rate was estimated for 20 W/cm2 and when crystal rotation and crucible rotation is 5 rpm, the maximum solidification length can be obtained and has a stable solidification.

Keywords: Liquid fraction; Silicon solidification; Czochralski crystal growth; Crucible rotation; Crucible wall heat flux

1. Introduction

The crystal growth process provides basic materials for many applications and this is one of the key technologies in all manufacturing processes for electronic devices. The semiconductor field is photovoltaic (PV) and this PV technique is very important to the next generation for solar cells because the solar electric power depends on PV production technique. T. Surek [1] reported on the progress in solar cell efficiency and this report contains that the final data point for 2003 corresponds to $3.00/watt and a cumulative capacity of 3000 megawatts and reaches the maximum efficiency of near 35%. The silicon wafer for solar cell is classified into two groups: the ribbon growth on substrate (RGS) and the other group is the horizontal ribbon growth (HRG) and vertical ribbon growth (VRG). These HRG [2] and VRG are based on the crystallization of silicon films of equal thickness on either side of a ribbon which is pulled vertically or horizontally along through silicon melt. But the RGS process has the crystallization of silicon films on one side of a ribbon. This RGS production technique has been introduced by many of researchers [2-5] and this study applied it. This RGS silicon wafer manufacturing technology is a very promising high speed wafer production technique and the effective production of silicon wafers at low manufacturing costs. To produce a good quality of thin silicon wafer, the solidification condition is very important and many researchers are concerned with the manufacturing condition and physical problems. J. H. Lim et al. [6] reported the thermal and materials characteristics on a thin silicon substrate.

The demand for large scale of silicon ingot has increased in recent days. For this purpose, single crystalline silicon is used as a basic raw material for the production, and the main bulk of the silicon for the electronic industry is produced by means of ingot pulled from the melt – t he Czochralski (CZ). The main problem of the technology is unstable melt convection that leads to the fluctuations of the growth rate, and the fluid flow is very complicated and difficult to catch thermal fluid phenomena. Many researchers are studying the thermal and fluid flow for solving the silicon melt flow and there are limitations to silicon ingot size. D. Franke [7] has reported the temperature distribution in furnaces and silicon ingots for

† This paper was recommended for publication in revised form by Associate Editor Jae Dong Chung

*Corresponding author. Tel.: +82 55 640 3185, Fax.: +82 55 640 3188
E-mail address: hschung@gnu.ac.kr

various process conditions and Enger [8] showed the time-dependent simulations of the flow and heat transfer in an identical crucible geometry. One of targets in the current research focuses on the production of large-diameter silicon wafer, for that purpose. Gorbunov [9] reported investigations concerning the physical modeling of Czochralski growth of silicon large-diameter single crystals and also employed actual criteria of the real process such as Reynolds and Grashof numbers. On the other hand, to get more stable and good quality in crystal silicon, some of papers present the case of the influence of magnetic fields. Virbulis [10] and Krauze [11] have reported the use of dynamic magnetic fields for the possibility to influence the melt movement, and they showed the effects by the crystal, crucible rotation and electromagnetic. The demand for large crystal diameter becomes more in semiconductor field and the development of this large crystal is very expensive.

As numerical modeling of the silicon melt flow has grown to becoming a successive and powerful tool, it can reduce development costs and shorten design cycles. To meet these technique demands, in this paper, the optimum solidification condition was investigated by the heat generation rate on the crucible wall, crucible rotation and crystal rotation, and also the solidification region was classified by these calculation parameters. Also, in this research work, the volume of fluid models (VOF) and thermal fluid flows with various parameters have been considered to find the optimum solidification conditions. These solidification conditions will be used to produce the silicon wafer with more economic process and low cost.

2. Numerical procedure and validation

Numerical simulations are performed with the FLUENT^{TM} software package and it is a finite volume (FVM) code, based on a structured multi domain grid approach and pressure-based solution algorithm according to the SIMPLE scheme. The calculation of flow field is based on the steady state solution for volume fraction, momentum and energy for an incompressible fluid. The Boussinesq approximation **is** used for buoyancy term. Volume of fluid (VOF) as a multiphase model has applied for the calculation of solidification, and implicit VOF scheme is used in this calculation.

The VOF model can model two or more immiscible fluids by solving a single set of momentum equations and tracking the volume fraction of each of the fluids throughout the domain. One of the governing equations for the VOF model is the volume fraction equation and the main concept is the following. The tracking of the interfaces between the phases is accomplished by the solution of a continuity equation for the volume fraction of one or more of the phases. For the qth phase, this equation has the following form:

$$\frac{1}{\rho_q}\left[\nabla\cdot(\alpha_q\rho_q\overline{v_q}) = \sum_{p=1}^{n}(\dot{m}_{pq}-\dot{m}_{qp})\right] \tag{1}$$

Where $\dot{m}_{qp}$ is the mass transfer from phase q to phase p and $\dot{m}_{pq}$ is the mass transfer from phase p to phase q. Two materials are used in this paper and phase p and phase q are corresponding to air and silicon, respectively. The qth fluid's volume fraction in the cell is denoted as α_q.

The momentum equation is solved throughout the domain, and the resulting velocity field is shared among the phases. The momentum equation, shown below, is dependent on the volume fractions of all phases through the properties ρ and μ.

$$\nabla\cdot(\rho\vec{v}\vec{v}) = -\nabla p + \nabla\cdot\left[\mu(\nabla\vec{v}+\nabla\vec{v}^{T})\right] + \rho\vec{g} + \vec{F} \tag{2}$$

The energy equation, also shared among the phases, is shown below.

$$\nabla\cdot(\vec{v}(\rho E + p)) = \nabla\cdot(k_{eff}\nabla T) + S_h \tag{3}$$

The VOF model treats energy, E, and temperature, T, as mass-averaged variables:

$$E = \frac{\sum_{q=1}^{n}\alpha_q\rho_q E_q}{\sum_{q=1}^{n}\alpha_q\rho_q} \tag{4}$$

Where Eq for each phase is based on the specific heat of that phase and the shared temperature. The properties ρ and k_{eff} (effective thermal conductivity) are shared by the phases and the source term, S_h represent the volumetric heat sources. In the case of turbulence quantities, a single set of transport equations is solved, and the turbulence variables are shared by the phases throughout the field. For the turbulence models, the Reynolds stress model is used in this paper. For simulations using the VOF multiphase model, upwind schemes are generally unsuitable for interface tracking because of their overly diffusive nature. Central differencing schemes, while generally able to retain the sharpness of the interface, are unbounded and often give unphysical results. To overcome these, the high resolution interface capturing (HRIC) scheme is used and this modified HRIC scheme provides improved accuracy for VOF calculations when compared to QUICK and second-order schemes or other schemes [12].

To include the effect of solidification/melting process, an enthalpy-porosity technique is used. In this technique, the melt interface is not tracked explicitly. Instead, a quantity called the liquid fraction, which indicates the fraction of the cell volume that is in liquid form, is associated with each cell in the domain. The liquid fraction is computed at each iteration, based on an enthalpy balance. The "mushy zone" is a region in which the liquid fraction lies between 0 and 1. The mushy zone is modeled as a "pseudo" porous medium in which the porosity decreases from 1 to 0 as the material solidifies. Here, the liquid fraction, β, is defined as:

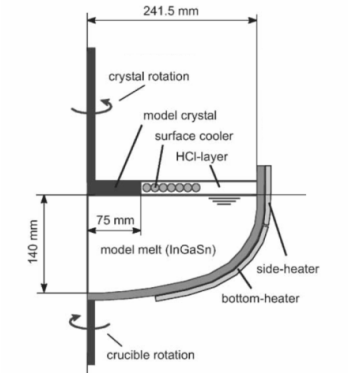

Fig. 1. Experimental setup for Czochralski silicon melt flow (T. Wetzel, 2001).

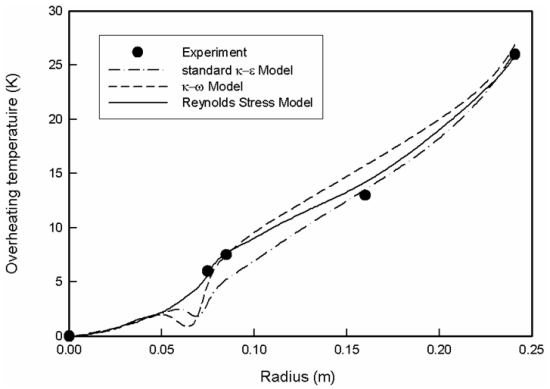

Fig. 2. Calculation validation with experimental data of reference in case of crystal rotation rate -15 rpm and crucible rotation rate 5 rpm (T. Wetzel, 2001).

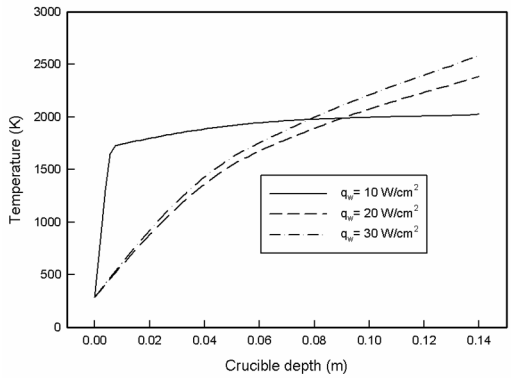

Fig. 3. Temperature distributions on centerline depth of crucible for various wall heat flux in case of *Rc*= -5rpm and *Rs*= 5 rpm.

$$\begin{aligned} &\beta = 0 \text{ if } T < T_{solidus} \\ &\beta = 1 \text{ if } T > T_{liquidus} \\ &\beta = (T - T_{solidus}) / (T_{liquidus} - T_{solidus}) \text{ if} \\ &T_{solidus} < T < T_{liquidus} \end{aligned} \quad (5)$$

Here, the liquid fraction, β can be calculated by the energy equation, and after the energy equation is solved some calculation cells change to solid cells with velocity zero. These results are coupled with the momentum equation and the cell conditions, such as solid or fluid parts are determined newly.

A good prediction of the solidification depends on the simulation temperature fields, but temperature measurements in molten silicon are very difficult, and the simulation tool is verified by comparisons of the experimental results [13]. This reference uses the fluid of eutectics InGaSn model melt, because this alloy has a melting point of 10.35˚C [9], which enable long-time measurements and the determination of temperature.

Fig. 1 shows the experimental setup by reference [13] and Fig. 2 represents the calculation results. The comparison results are based on mean temperature values determined in certain points along a radial line by 5 mm beneath the free surface. All temperature values were transformed into temperature differences with respect to a reference point. This reference point is the measuring point on the axis. It is the point closet to the minimum temperature along the crystal wall, and so all the calculated temperature differences can be regarded as overheating temperatures. From Fig. 2, the numerical results by Reynolds stress model had a good agreement with experimental data.

3. Results and discussion

To obtain the optimum solidification and the effects between the crystal rotation and crucible rotation, the same geometry with Fig. 1 was used in numerical analysis. A crucible of 483mm in diameter is filled with silicon melt as high as 140mm. A heat flux on the crucible outside surface has been set to 10, 20 and 30 W/cm^2 and a crystal model, 150mm in diameter, has been set to a constant temperature of 288K; the liquid silicon is crystallized near the crystal rotation disc, and it can be controlled by the heat flux and rotations of the physical model.

The silicon melt free surface, which is the free surface except for the crystal rotation disc as shown Fig.1, has a boundary condition of free stream temperature of 2000K and convective heat transfer coefficient of 100 W/m^{2}K. The crystal rotation, *Rc* and the crucible rotation, Rs were set to a range of 0 to 20 rpm. Constant physical property values for silicon were used in calculations: dynamic viscosity η=0.00086 kg/(ms), density ρ=2530 kg/m^3, melting point temperature T_m=1688K, solidus temperature T_s=1663K, liquidius temperature T_l =1713K, thermal conductivity k=67 W/ (m-K), and specific heat capacity Cp=716 J/ (kg-K). Fig. 3 shows the temperature distributions on centerline depth of crucible for various wall heat flux in case of *Rc*= -5rpm and *Rs*=5, and also each figure has the parameters of heat fluxes, q_w= 10, 20 and 30 W/cm^2. As the heat flux increases, the temperature distribution is changed smooth, but a small heat flux of q_w= 10W/cm^2 has an abrupt change of the temperature near the crystal rotation disc. This can show that the heat generation on crucible wall is not dominant compared to the cooling effect from the crystal rotation disc. The same phenomenon occurs in the liquid fraction distributions as shown in Fig. 4. When

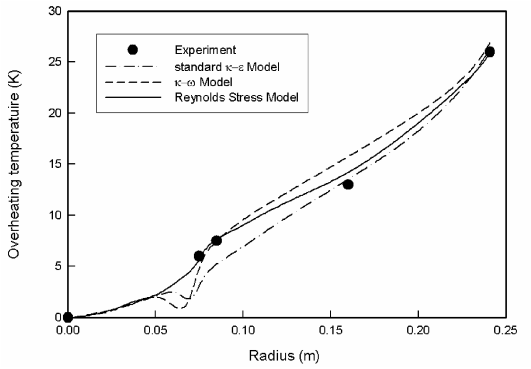

Fig. 4. Liquid fraction distributions on centerline depth of crucible for various wall heat flux in case of *Rc*= -5 rpm and *Rs*= 5 rpm.

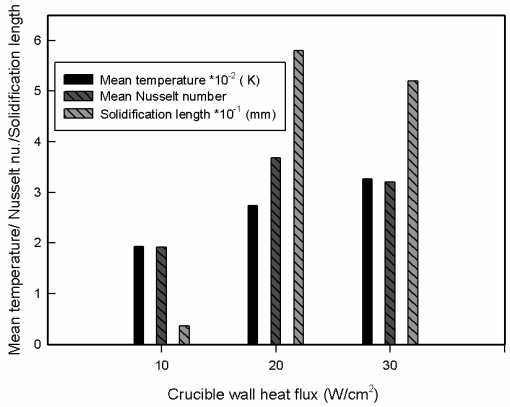

Fig. 5. Mean temperature, Nusselt nu. and solidification length according to crucible wall heat flux in case of *Rc*=-5 rpm and *Rs*= 5 rpm.

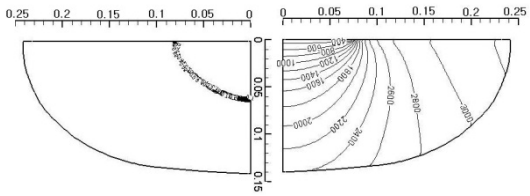

Fig. 6. Liquid fraction and temperature contours in case of *Rc*= -5 rpm and *Rs*= 5 rpm with q_w= 20 W/cm^2.

the heat flux is greater than 20 W/cm^2, the liquid fraction has not changed much. The value of liquid fraction such as Fig. 4 is between 0 and 1, and the solid state represents 0 and fluid state has a value of 1.

Fig. 5 represents the mean temperature, mean Nusselt number and solidification length according to crucible wall heat flux in case of *Rc* = -5 rpm and *Rs*=5 rpm. The mean temperature is the area based mean temperature inside of the calculation domain; the mean Nusselt number shows the value at the crucible wall, and the solidification length shows the solid state length. As the crucible wall heat flux increases, q_w=10-30W/cm^2, the mean temperature increases with a range of 2000 to 3000K. This mean temperature is a general phenomenon, but the changes of Nusselt number and solidification length with crucible heat flux have different patterns. The case

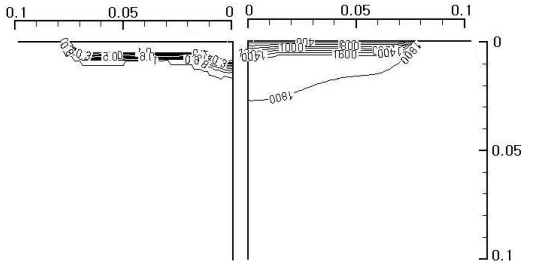

(a) *Rc*= -5 rpm, *Rs*= 2.5 rpm

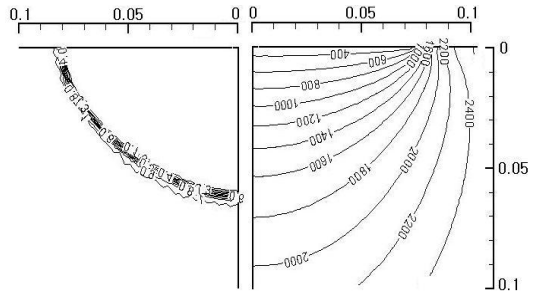

(b) *Rc*= -5 rpm, *Rs*= 5 rpm

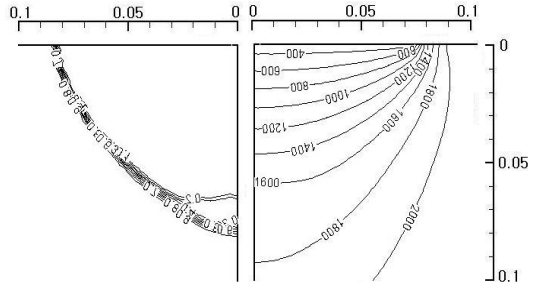

(c) *Rc*= -5 rpm, *Rs*= 7.5 rpm

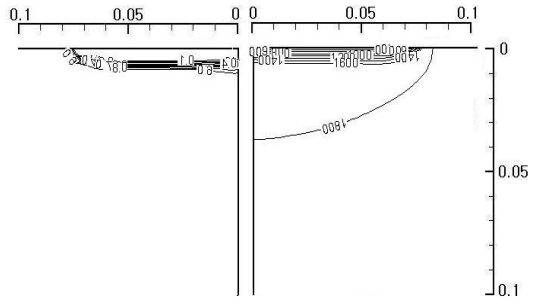

(d) *Rc*= -5 rpm, *Rs*= 10 rpm

Fig. 7. Changes of liquid fraction and temperature contours for various Rs with q_w= 20 W/cm^2.

of q_w=20 W/cm^2 shows the maximum values of Nusselt number and solidification length. This means that the heat transfer is high and more large scale solidification can be produced, and we can conclude that the economic crucible wall heat flux is 20 W/cm^2.

Fig. 6 represents the liquid fraction and temperature contours in case of *Rc*= -5 rpm and *Rs*= 5 rpm with q_w=20 W/cm^2. From the left figure of Fig. 6, the crystal formation is clear and has about 60mm in diameter. The right figure of Fig. 6 shows

the temperature contours and has more dense temperature distributions near the crystal rotation disc; the maximum temperature is shown at the right top corner because of centrifugal force by crucible rotation.

Fig. 7 show the changes of liquid fraction and temperature contours for various crucible rotation, *Rs* with q_w= 20 W/cm^2. These figures are drawn near the crystal rotation disc because of understanding the crystallization. The solidification process is changed to the crucible rotation and most stable solidification is found in case of *Rc*= -5 rpm and *Rs*= 5 rpm; this solidification boundary is formed at the solidus temperature of T_s=1663K. These temperatures and liquid fractions of variation to crucible rotation are shown Fig. 8 and Fig.9. The temperature and liquid fraction in case of *Rc*= -5 rpm and *Rs*= 5 rpm shows the most smooth and best solidification process.

Fig. 10 shows the mean temperature inside the crucible for various crucible rotation rates in case of Rc= -5rpm and q_w= 20 W/cm^2. The maximum temperature is found at crucible rotation of Rs=5 rpm, which means that the most active heat transfer is occurring on the crucible wall compared to other crucible rotation in spite of the same heat flux of the crucible wall. Fig. 11 shows the changes of liquid fraction and temperature contours for increasing *Rc* and *Rs* with q_w=20 W/cm^2. When there is no rotation, the solidification is better than the case of large rotation such as 15 rpm, but it becomes worse than 5 rpm. Comparing the 1600K isotherm in Fig. 11, it can be seen that this contour is closer near crystal disc than case Fig. 11(b) and (c). This is because the heat transfer from the crucible wall is not affecting the crystal. Fig. 12 and Fig. 13 show the temperature and liquid fraction distributions on centerline depth of crucible for various revolution rates in case of q_w=20 W/cm^2.

As the revolutions increase in Fig. 11(b), (c) and (d), the temperature gradient in the solidified region is large near the crystal rotating disc and the solid silicon area becomes smaller. Increasing the revolution of the crucible reduces the effects of the heat generation from the crucible wall. This Czochralski growth of silicon has two rotating mechanisms such as crystal and crucible rotation in Fig. 1, and these rotating forces can affect the crystallization of silicon. The diameter in the crystal rotation disc is smaller than that of the crucible and the effect of rotation on the silicon melt cannot spread to the silicon melt. Conversely, the crucible rotation effects are more dominant on the silicon melt and this can change the temperature profiles and lead to changes of the liquid fraction. If the crucible rotation is higher than 15 rpm in Fig. 11(d), the temperature gradient will be denser at near crystal rotation disc and the liquid fraction area becomes smaller. An excessive rotation of the crucible causes a large centrifugal force and this becomes like a barrier which interrupts the propagation of high temperature from crucible to the center of the crucible.

Fig. 14 shows the mean temperature inside the crucible for various crucible rotation rates in case of q_w=20 W/cm^2. There is a distinct point at *Rs*=5 rpm which shows the maximum mean temperature. Increasing the crucible rotation reduces the

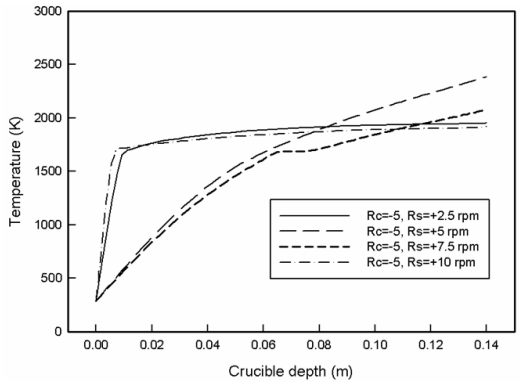

Fig. 8. Temperature distributions on centerline depth of crucible for various rotation rate in case of q_w=20 W/cm^2.

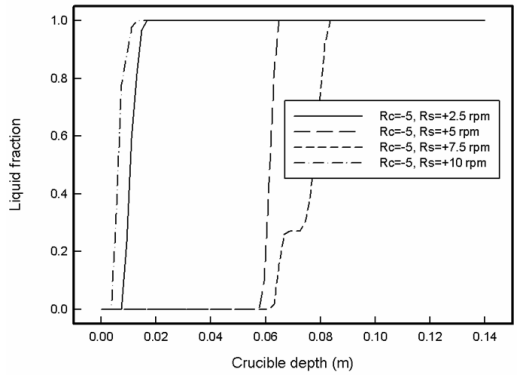

Fig. 9. Liquid fraction distributions on centerline depth of crucible for various rotation rate in case of q_w= 20 W/cm^2.

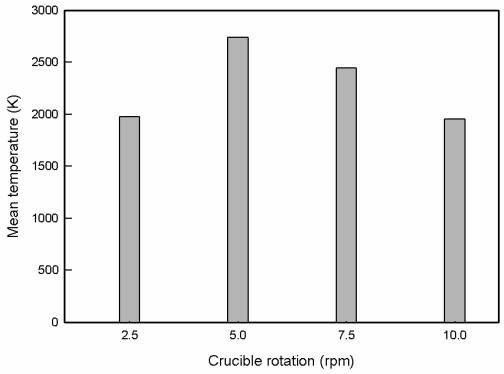

Fig. 10. Mean temperature of inside crucible for various crucible rotation rates in case of *Rc*=-5rpm and q_w=20 W/cm^2.

mean temperature, but the mean temperature is constant more than crucible rotation *Rs*=25 rpm. This indicates that the heat transfer from the crucible wall does not expand to the center of the crucible because of exceeding centrifugal force.

A plot of solidification depth as a function of crucible rotation is given in Fig. 15. This figure shows that the maximum solidification depth of 58mm is found at a crucible rotation of 5 rpm. Even if there is no rotation, the solidification depth shows about 35mm, but increasing the rotation to 2.5 rpm, the solidification depth is decreased under 5mm rapidly. When

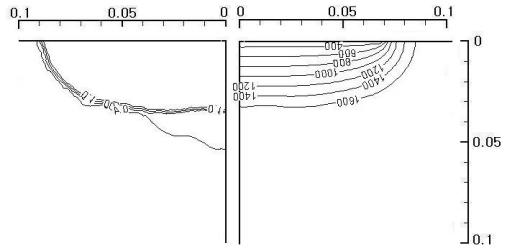

(a) *Rc*= -0 rpm, *Rs*= 0 rpm

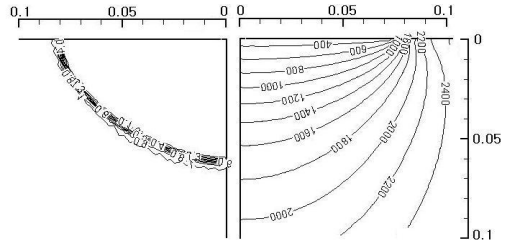

(b) *Rc*= -5 rpm, *Rs*= 5 rpm

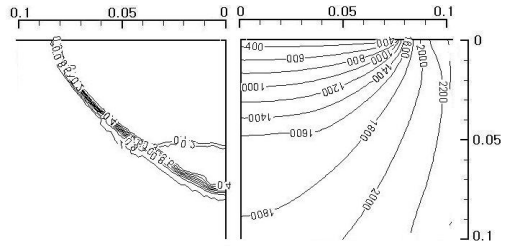

(c) *Rc*= -10 rpm, *Rs*= 10 rpm

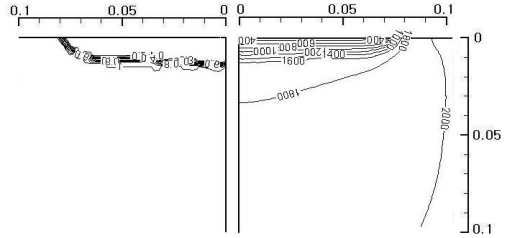

(d) *Rc*= -15 rpm, *Rs*= 15 rpm

Fig. 11. Changes of liquid fraction and temperature contours for increasing *Rc* and *Rs* with q_w= 20 W/cm^2.

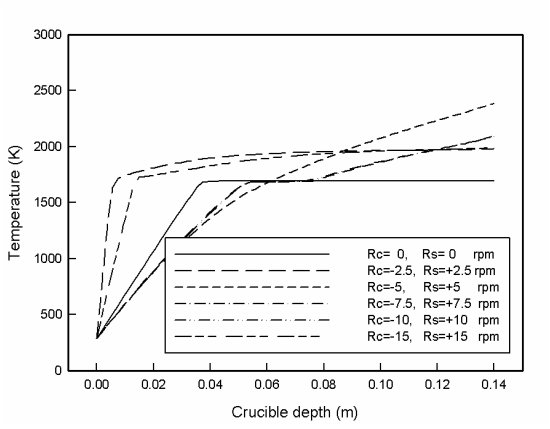

Fig. 12. Temperature distributions on centerline depth of crucible for various revolution rates in case of q_w=20 W/cm^2.

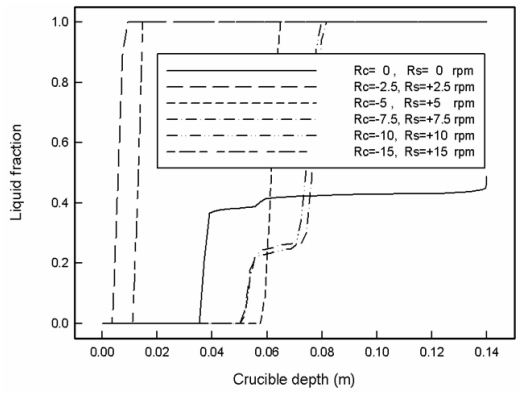

Fig. 13. Liquid fraction distributions on centerline depth of crucible for various revolution rates in case of q_w=20 W/cm^2.

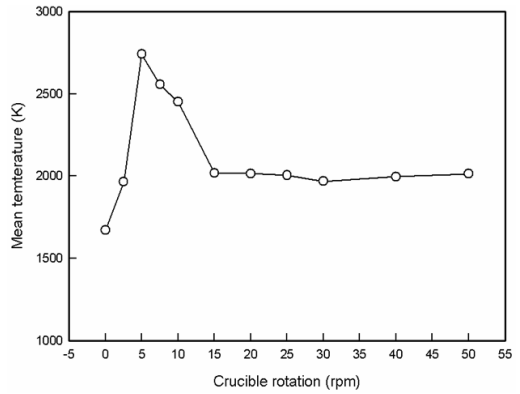

Fig. 14. Mean temperature of inside crucible for various crucible rotation rates in case of q_w=20 W/cm^2.

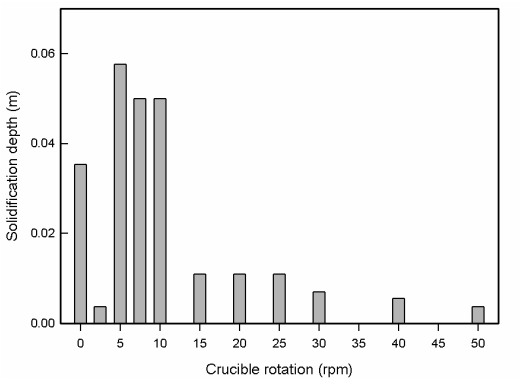

Fig.15. Solidification depth for various crucible rotation rates in case of q_w=20 W/cm^2.

the rotation is increased again the maximum solidification depth of 58mm is found at a crucible rotation of 5 rpm. This means that the rotation rates can strongly affect the solidification condition. For the range over 15 rpm, the solidification depth is not changed and is almost same with about 10mm; this phenomenon is related to the mean temperature of Fig.14. Therefore, an exceeding crucible rotation isolates the propagation from heat generation on crucible to the center of the crystal rotation disc.

4. Conclusions

The Czochralski crystal process is a powerful method for silicon wafer manufacturing, and this process or performance depends on the crucible rotation factors. The thermal and fluid condition of the Czochralski crystal process is very important; when there is no rotation of the crucible the natural convection is dominant, so the melt silicon with high temperature moves to the center along the surface. As the crucible has some rotation, the melt silicon cannot move to the center because of centrifugal force and a good solidification condition can be obtained. This reason is why the crucible rotation factors are significant in the Czochralski crystal process.

Thus, to get economic solidification conditions, a numerical analysis has been carried out by using various parameters such as crucible rotations, crystal rotations and heat generation rates on crucible wall. The crystal revolution rates, *Rc* , are set in the range of 0 to -15 rpm, and the crucible revolution rates, *Rs,* are set in the range of 0 to 50 rpm; the heat fluxes rates on crucible wall, q_w are changed to 10 to 30 W/cm^2 for the main calculation parameters.

The economic heat flux is estimated as 20 W/cm^2 and this condition has the maximum solidification depth and the maximum mean Nusselt number. It is shown that the changes of crucible rotations highly affect the silicon solidification process rather than that of crystal rotation, which is installed at the center of the crucible.

Therefore, the effective method for the process of wafer manufacturing is not to adjust the crystal rotation but to control crucible rotation. The crucible rotation of *Rc*= 5 rpm and crystal rotation of *Rc*= -5 rpm are considered as the economic solidification conditions for silicon wafer manufacturing.

From the comparison of no-crucible rotation and with crucible rotation, the case of crucible rotation of 5 rpm has almost twice the solidification effect. This is why the crucible rotation is important in silicon wafer manufacturing process and these conditions will be used for a more economic process and lower cost.

Acknowledgment

This work has been supported by the Brain Korea 21 Project and financially supported by Ministry of Education, Science Technology (MEST) and Korea Institute for Advancement of Technology (KIAT) through the Human Resource Training Project for Regional Innovation, and the authors gratefully appreciate the support.

References

[1] Thomas Surek, Crystal growth and materials research in photovoltaics: progress and challenges, *Journal of Crystal Growth 275* (2005) 292-304.

[2] I. Steinbach and M. Apel, Phase-field simulation of rapid crystallization of silicon on substrate, *Materials Science and Engineering A,* 449-451 (2007) 95-98.

[3] A. Burger, A. Gutjahr, L. Laas, A. Schönecker, S. Seren and G. Hahn, Near 13% efficiency shunt free solar cells on RGS wafers, *2006 IEEE 4th World Conference on Photovoltaic Energy Conversion*, (2006) 1-4.

[4] S. Seren, G. Hahn, A. Gutjahr, A.R. Burgers, A. Schönecker, A. Grenko and R. Jonczyk, Ribbon growth on substrate and molded wafer-two low cost silicon ribbon materials for PV, *2006 IEEE 4th World Conference on Photovoltaic Energy Conversion*, (2006) 1330-1333.

[5] G. Hahn, C. Zechner, B. Bitnar, M. Spiegel, W. Jooss, P. Fath, G. Willeke, E. Bucher and H.-U. Höfs, Solar cells with 11% Efficiency on Ribbon-Growth-on-Substrate (RGS) Silicon, *Prog. Photovolt. Res. Appl*. 6 (1998) 163-167.

[6] J. H. Lim1, M. H. Han, J.-Y. Lee, Y. Y. Earmme, S.-b. Lee and S. Im, A Study on the thermomechanical behavior of semiconductor chips on thin silicon substrate, *Journal of Mechanical Science and Technology*, 22 (2008) , 1483-1489.

[7] D. Franke, T. Rettelbach, C. Häβler, W.Koch and A. Müller, Silicon ingot casting: process development by numerical simulations, *Solar Energy Materials & Solar Cells,* 72 (2002) 83-92.

[8] Sven Enger, Oliver Gräbner, Georg Müller, Michael Breuer and Franz Durst, Comparison of measurement and numerical simulations of melt convection in czochralski crystal growth of silicon, *Journal of Crystal Growth,* 230 (2001) 135-142.

[9] L. Gorbunov, A. Pedchenko and A. Feodorov, Investigation of temperature field and melt flows in large diameter CZ silicon modeling experiments with impact of magnetic fields, *Int' Scientific Colloquium Modeling for Electromagnetic Processing*, Hannover, Mar. 24-26 (2003) 317-322.

[10] J. Virbulis, Th. Wetzel, A. Muiznieks, B. Hanna, E. Dornberger, E. Tomzig, A. Muhlbauer and W.v. Ammon, Numerical investigation of silicon melt flow in large diameter CZ-crystal growth under the influence of steady and dynamic magnetic fields, *Journal of Crystal Growth* 230 (2001) 92-99.

[11] A. Krauze, A. uiznieks, A. Muhlbauer, Th. Wetzel, L. Gorbunov, A. Pedchenko and J. Virbulis, Numerical 2D modelling of turbulent melt flow in CZ system with dynamic magnetic fields, *Journal of Crystal Growth* 266 (2004) 40-47.

[12] Jang O. Mo, 2008 *ATES CFD/CAE Conference*: Korea ANSYS Users' Meeting, (2008) 44.

[13] Th. Wetzel, A. Muiznieks, A. Muhlbauer, Y. Gelfgat, L. Gorbunov, J. Virbulis, E. Tomzig and W.v. Ammon, Numerical model of turbulent CZ melt flow in the presence of AC and CUSP magnetic fields and its verification in a laboratory facility, *Journal of Crystal Growth* 230 (2001) 81-91.

Hyo-Min Jeong received his Ph.D. degree from the University of Tokyo, Japan in 1992, respectively. Dr. Jeong is currently a Professor at the Department of Mechanical and Precision Engineering at Gyeongsang National University in Tongyeong, Korea. His research interests include fluid engineering, CFD, cryogenic systems, ejector systems, mechanical vapor compression, and cascade refrigeration system.s.

Han-Shik Chung received his Ph.D. degree from Donga University, Korea in 1987. Dr. Chung is currently a Professor at the Department of Mechanical and Precision Engineering at Gyeongsang National University in Tongyeong, Korea. His research interests include thermal engineering, heat transfer, LNG vaporizer optimum, solar cells, and fresh water systems from sea water.